Formation of Low−Density Water Clusters in the Silicalite1 Cage: A Molecular Dynamics Study

ARTICLE *in* THE JOURNAL OF PHYSICAL CHEMISTRY B · NOVEMBER 2003

Impact Factor: 3.3 · DOI: 10.1021/jp035151d

4 AUTHORS, INCLUDING:

Siegfried Fritzsche
University of Leipzig
101 PUBLICATIONS **1,035** CITATIONS
SEE PROFILE

Reinhold Haberlandt
University of Leipzig
60 PUBLICATIONS **779** CITATIONS
SEE PROFILE

Supot Hannongbua
Chulalongkorn University
124 PUBLICATIONS **1,284** CITATIONS
SEE PROFILE

Formation of Low-Density Water Clusters in the Silicalite-1 Cage: A Molecular Dynamics Study

Chuenchit Bussai,[†,‡] Siegfried Fritzsche,[‡] Reinhold Haberlandt,[‡] and Supot Hannongbua*[,†]

Department of Chemistry, Faculty of Science, Chulalongkorn University, Bangkok 10330, Thailand, and Department of Molecule Dynamics/Computer Simulations, Faculty of Physics and Geoscience, University of Leipzig, Linnéstr.5,04103, Leipzig, Germany

Received: April 28, 2003; In Final Form: August 26, 2003

A series of molecular dynamics simulations have been performed to examine changes to the structural and dynamical properties of water molecules in silicalite-1 as a function of temperature and loading. The ab initio fitted silicalite-1/water potential which is newly developed[18] and the BJH flexible water/water potential[15] have been employed. The water loading was varied from 1 to 8 water molecules per intersection, equivalent to 8−64 molecules per simulation cube. The simulations have been carried out at 298 and 393 K. The results show that the water structure inside the silicalite-1 cages changes dramatically as a function of loading. We found that the probability of water molecules residing in a straight channel is always higher than that of residing in the sinusoidal channels. Under high loading, the observed clusters form a structure similar to that of pure water. We call it a "low-density cluster" for the following reasons: (i) The cluster consists of five water molecules (four in the first hydration shell of the central one) which is consistent with that of pure water. (ii) However, molecules in the cluster are not coordinated together via hydrogen bonds. The radius of the first hydration shell of 3.35 Å is 0.5 Å longer than that of pure water. (iii) Molecules in the cluster are less flexible than those of pure water. In terms of dynamical properties, for low loadings, a preferential diffusion path is observed along the center of the channel tube. The water molecules were detected to diffuse closer to the surface when the concentration was higher than six molecules per intersection. The diffusion coefficient of water decreases when the concentration increases. The *D* values for all concentrations at 393 K are higher than those at 298 K. The temperature dependence almost disappears at a loading of eight water molecules per intersection. In addition, the anisotropic diffusion is less pronounced for water in silicalite-1 in comparison to that of nonpolar molecules.

1. Introduction

It is a well-known fact that structural properties of guest molecules in zeolite cages or other microporous materials are directly related to the macroscopic properties of the system. Changes of microscopic characteristics in terms of formation and deformation of molecular clusters—dimers, trimers, and so forth—can significantly influence those system properties and hence their applications in industrial processes.[1−3] This matter has attracted the attention of both basic and applied researchers. However, such microscopic characteristics cannot be measured by experimental techniques because of the complex interplay between many physical and chemical processes taking place in the zeolites. Therefore, molecular dynamics simulations are the leading tools for obtaining insight into the microscopic details.

Despite the fact that even small amounts of water, one of the most common substances found in zeolites, can significantly influence properties of zeolite-like materials during some technological processes and can also have effects on the adsorption of other molecules,[4,5] so far only little information is available. To the best of our knowledge, most of the molecular dynamics simulations for water in zeolites have been reported by Demontis et al.[6,7] and Leherte et al.[8,9] In the late 1990s, the sodium ions in hydrated zeolite A were examined over different ranges of hydration.[10] The self-diffusion coefficient at full hydration obtained from that simulation is 3 times higher than that obtained from experiments. More recently, empirical potential functions, including electronic field dependent terms, have been developed and applied by Cicu et al.[11] to classically simulate water in natrolite. It was found that the electric field dependent terms in the intramolecular potential of water can improve the results in comparison with experiment. Termath et al.[12] have performed ab initio molecular dynamics simulations (AIMD) for H_2O and H_3O^+ in HSAPO-34 and detected the water cluster, $H_3O^+(H_2O)_2$ (i.e., an acid−base reaction), in HSAPO-34, which requires at least three water molecules per two nearby acidic sites. However, AIMD simulations are still computationally demanding. This restricts calculations to systems with at most a few hundred atoms and restricts the typical run length to some picoseconds. For the de-aluminated zeolite silicalite-1, the only available data are in terms of heat of adsorption. Vigné-Maeder and Auroux[13] have drawn a potential map in which the average energy is expressed as a sum of electrostatic, polarization, dispersion, and repulsion interactions between the atom pairs. The calculations yield a heat of adsorption for water in silicalite-1 at 300 K of -12.5 kcal·mol^{-1}. More recently, Turov et al.[14] have measured the water adsorption in silicalite-1 by ^{1}H NMR and thermogravitric methods and observed a high chemical shift. This corresponds to the formation of more than three hydrogen bonds of the attributed water in the pores.

* To whom correspondence should be addressed. E-mail: supot.h@chula.ac.th.
† Chulalongkorn University.
‡ University of Leipzig.

10.1021/jp035151d CCC: $25.00
Published on Web 10/11/2003

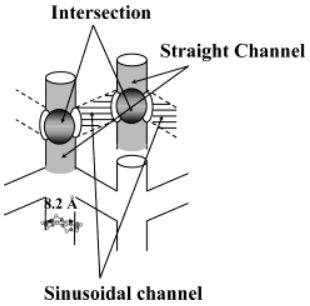

Figure 1. Schematic representation of silicalite-1 channels.

In fact, all previous classical simulations[6−11,13] of water in zeolites use intermolecular potentials based on empirical force-field parametrizations. Some doubts arise when the potentials are used to represent the interaction between water and zeolites in which hydrogen bonding is very important, as this is better represented by ab initio derived potentials. Such potentials are therefore used in the present paper. In addition, the water−water interaction is represented by an existing potential,[15] which is mainly fitted to ab initio data. It is well known that an imbalance in the water−zeolite and water−water pair potentials can easily lead to artificial results. To avoid this discrepancy, an ab initio fitted potential for water/silicalite-1 has been developed for the first time using fairly large fragments of 10T, 20T, and 27T of silicalite-1, where T refers to silicon atoms of corner-sharing TO_4 tetrahedra in the zeolite crystalline.[16] The ab initio fitted force field has been applied to the study of diffusion coefficients of water in silicalite-1 and is found to be in satisfactory agreement with those observed using PFG-NMR measurements.[5] Recently, dynamical and structural behavior of water molecules coverage in silicalite-1 at the range 100−580 K has been reported by Demontis et al.,[17] as a result of the molecular dynamics simulation using an electric field dependent potential.[11] At very low temperatures (below 225 K), solidlike clusters were revealed. Interestingly, a liquidlike behavior is exhibited in silicalite-1 channels in the intermediate temperature range 225−350 K, where the vaporlike features are evidently found.

In this paper, we present dynamical and structural properties of water molecules inside the siliceous ZSM-5 at various loadings with the aim of achieving an understanding at the molecular level. The ab initio fitted water/silicalite-1 model[18] based on quantum chemical methods has been employed.

2. Computational and Calculation Details

2.1. Structure of Silicalite-1. The silicalite-1 crystal structure used in the present investigation is characterized by a three-dimensional channel system, whose symmetry group is *Pnma*. Its framework structure incorporates two different channel systems, each defined by 10-oxygen-membered rings. A straight channel, with an elliptical cross section of about 5.2−5.7 Å, is parallel to the crystallographic axis *b*, while sinusoidal channels, with an almost circular cross section of 5.4 Å, run along the crystallographic axis *a* (Figure 1). The resulting intersections are stretched out to cavities of up to 9 Å in diameter. The crystallographic cell[19] contains 288 atoms ($Si_{96}O_{192}$), with lattice parameters $a = 20.07$ Å, $b = 19.92$ Å, and $c = 13.42$ Å.

2.2. Potential Functions. The potential proposed by Bopp et al.[15] was employed to describe water−water interactions and internal degrees of freedom of the water molecules. These functions were originally developed from the central force model by Lemberg and Stillinger.[20,21] The binding energy of water dimer of −5.6 kcal·mol^{-1} is in excellent agreement with experimental data, −5.4 to −5.5 ± 0.7 kcal·mol^{-1}. [22]

To develop the ab initio fitted silicalite-1/water pair potential, almost 1000 data points at the Hartree−Fock (HF) 6-31G* level have been calculated and fitted to the functional form[5,18] shown in eq 1:

$$\Delta E(\mathrm{w,s}) = \sum_{i}^{3}\sum_{j}^{288}\left\{\frac{A_{ij}^{ab}}{r_{ij}^{6}} + \frac{B_{ij}^{ab}}{r^{12}{}_{ij}} + \frac{C_{ij}^{ab}}{r_{ij}^{3}} + \frac{Qq_iq_j}{r_{ij}}\right\} \quad (1)$$

where 3 and 288 denote the numbers of atoms in a water molecule (w) and the silicalite-1 (s) unit cell, respectively. The constants A_{ij}, B_{ij}, and C_{ij} are fitting constants and r_{ij} is the distance between atom *i* of water and atom *j* of silicalite-1. Also, q_i and q_j are the atomic net charges of atoms *i* and *j* in atomic units, obtained from the population analysis[23] of the isolated molecules in the quantum chemical calculations (more details see ref 18) while $Q = 332.05$ is a constant, required to change Coulombic interaction from atomic unit to kcal·mol^{-1}. Superscripts a and b on the fitting parameters have been used to classify atoms of equal atomic number but different environmental conditions, for example, oxygen and silicon atoms of silicalite-1 in the different channels. The third polynomial term ($C_{ij}/r^3{}_{ij}$) was added to obtain better numerical fitting. The contribution from this term at the cutoff distance, 10 Å (see section 2.3), is almost negligible (more details see ref 16). The fitting parameters are summarized in Table 1.

Discrepancies and reliabilities of the energy points because of the calculation methods and the basis sets used as well as the imbalance of the basis set, basis set superposition error, have been intensively examined.[16] The most stable silicalite-1/water interaction energy (in the configuration in which the water molecule lies at the center of the intersection) of −4.5 kcal·mol^{-1} obtained from the HF/6-31G* calculation is slightly different from that of −3.8 kcal·mol^{-1} from the correlated MP2 method with the same basis set.[16] However, the shape of the pair potential and changes in interaction energy as a function of separation from both methods are almost identical. More detailed discussion is provided elsewhere.[16] Unfortunately, an experimental value is not available for this system.

2.3. Molecular Dynamics Simulations. The equations of motion were integrated using the Velocity Verlet algorithm[24] with a time step of 0.5 fs at 298 and 393 K. Simulations[25] have been performed for systems containing 1−8 water molecules per intersection, equivalent to 8−64 molecules per simulation cube, which contains two silicalite-1 unit cells. The NVT ensemble was employed after 5 ps, when the velocities of the particles were rescaled to thermalize the system. Periodic boundary conditions were applied. The pair interactions were computed in the minimum image convention with a spherical cutoff of 10 Å. The length of each trajectory was 10 ns. The fluctuations of the total energy of the system were less than 0.005%. For the long-range Coulombic interactions, the shifted force strategy, which is successfully used in recent studies,[5,11,16−18] has been employed. Hence, Ewald summations can be avoided in this study in which the total charge of the system is zero.[26,27]

It has been found that lattice vibrations play a significant role only for the system of high activation energy, that is, size of the diffusive sorbate is relatively large in comparison to the window size.[25,28] For the investigated system, the activation energy for a single water molecule entering the silicalite-1 channel on the basis of HF/6-31G* calculation of −0.9 kcal·mol^{-1} [16] is much lower than that of about −8.0 kcal·mol^{-1} obtained from simulations using the empirical model.[13] In addition, the radius of water molecule of approximately 1.6 Å is very small in comparison to a pore radius of about 8.2 Å.

TABLE 1: Optimal Fitting Parameters for Atom *i* of Water Interacting with Atom *j* in Each Channel of the Silicalite-1 Lattice[a]

i	*j*	q_i	q_j	*A* (Å^6 kcal·mol^{-1})	*B* (Å^{12} kcal·mol^{-1})	*C* (Å^3 kcal·mol^{-1})
O	Si_{sd}	−0.87	1.57	− 9043.97	1161167.97	1418.92
O	Si_{st}	−0.87	1.67	− 4159.83	989963.68	617.02
O	O_{sd}	−0.87	−0.785	1371.19	−21045.58	−351.61
O	O_{st}	−0.87	−0.835	−110.79	51208.44	−110.82
H	Si_{sd}	0.435	1.57	3724.97	−4314.90	−792.37
H	Si_{st}	0.435	1.67	2077.13	−8925.29	−415.82
H	O_{sd}	0.435	−0.785	−406.18	689.37	222.32
H	O_{st}	0.435	−0.835	34.87	32.84	102.59

[a] Subscripts sd and st denote sinusoidal (zigzag) and straight channels, respectively; energies in kcal·mol^{-1}, distances (r_{ij}) in Å, and atomic net charges (q) in atomic units.

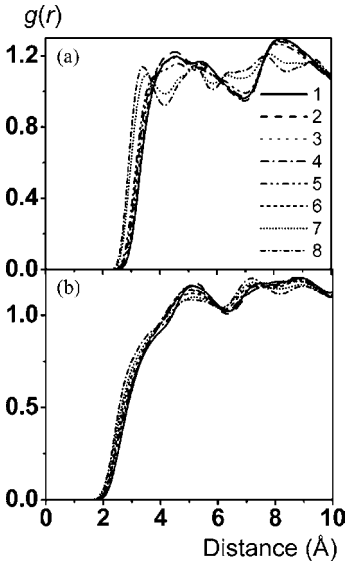

Figure 2. Radial distribution functions, $g(r)$, from oxygen atoms of silicalite-1 surface to (a) oxygen and (b) hydrogen atoms of water molecules at various loadings ($n_{ld} = 1-8$).

Therefore, this study was performed using rigid framework with flexible water model.

3. Results and Discussions

3.1. Structural Properties. 3.1.1. Silicalite−Water Radial Distribution Function (RDF). 3.1.1.1. Averaged RDF for All Channels. To investigate the structural data of water molecules via diffusion in zeolite silicalite-1 at various loadings (n_{1d}), the radial distribution functions (RDFs) from a surface oxygen atom (O_S) to oxygen (O_W) and hydrogen (H_W) atoms of water have been evaluated and plotted in Figure 2. The change of the water behavior is indicated by the O_S-O_W RDFs in which the transition takes place between the loadings of 6 and 7 water molecules per intersection.

The O_S-O_W RDFs for $n_{1d} \leq 6$ display first a broad maximum around 4.2 Å, followed by a pronounced shoulder at around 5.8 Å, and a second broad peak centered at 8.4 Å (Figure 2a). Because of the cylindrical structure (diameter 8.2 Å) (Figure 1) of the silicalite-1 channels, water molecules described by the first maximum and the established shoulder of the O_S-O_W RDFs can be assigned to molecules moving along the center of the tube. The distances from O_W to O_S of the nearest 10-oxygen-membered ring and their adjacent rings are between 4 and 6 Å. This is in good agreement with that predicted by ab initio calculations which state that the central line is the optimal path for a water molecule to travel along the silicalite-1 channels.[16]

A transition takes place for $n_{ld} > 6$, in which the first broad O_S-O_W peak splits into two sharp peaks centered at 3.45 Å and 5.25 Å. This feature indicates dramatic changes of the water behavior in silicalite-1 channels. With concentrations of more than six water molecules per intersection, the water molecules are forced by their repulsion to stay out of the central line region. This information cannot be obtained from ab initio calculations because only the interaction of a pair or only a few molecules can be taken into consideration. It is interesting to note here, therefore, that these two peaks are contributed by the same set of water molecules because the sum of O_S-O_W distances for O_W centered at 3.45 Å from O_S on one side and 5.25 Å from the opposite side of the 10-oxygen-membered ring is closed to the 8.2 Å diameter of the tube.

Concerning the appearance of the O_S-O_W peak at 3.45 Å for $n_{1d} > 6$, such a sharp, pronounced, and discrete peak is usually associated with a tight binding between the molecules. This is surely not true for the water/silicalite-1 system in which the interaction energies derived from ab initio calculations or the ab initio fitted potential of about −4.5 kcal·mol^{-1} for any configuration where the O_S-O_W distance is 3.45 Å is almost equal to that at the optimal configuration of the water dimer of −5.6 kcal·mol^{-1}, that is, the water−water binding is superior to the surface−water binding. Therefore, the formation of this peak can be assigned to a water cluster formation. Repulsion among molecules in the cluster within the limited space inside the silicalite-1 channels leads not only to a shift of water positions away from the middle of the channel but also to greater confinement of their positions. As a consequence of the cluster formation and the repulsion of the water molecules in a limited space, the O_S-O_W RDF starts to be detected at a shorter distance as the concentration increases. An investigation and discussion of the cluster formation is given in more detail in the next section.

In Figure 2b, we show the O_S-H_W RDF. The plots for all loadings show corresponding RDFs with established shoulders around 3.2 Å and a first pronounced maximum at around 5.2 Å. The following conclusions can be made regarding loading: (i) The appearance of the first pronounced O_S-H_W shoulder at a shorter distance than that of the first peak for O_S-O_W implies that water molecules point hydrogen atoms toward the inner surface of silicalite-1. (ii) With the distances to the first peak of the O_S-O_W RDFs of 3.45 Å and to the O_S-H_W shoulder of both peaks mentioned earlier, it can be concluded that hydrogen bonding between water molecules and the inner surface of silicalite-1 cannot be formed. (iii) The broadness of these peaks and their shoulders indicate a flexibility of water molecules in terms of both their positions and orientations. This finding confirms the ab initio results, which suggest changes of water orientations during diffusion along the silicalite-1 channels.[16] (iv) As with the O_S-O_W RDFs, the O_S-H_W RDFs for low loadings start to be detected at longer distances than those of high loadings. This is also true for the distance to the first

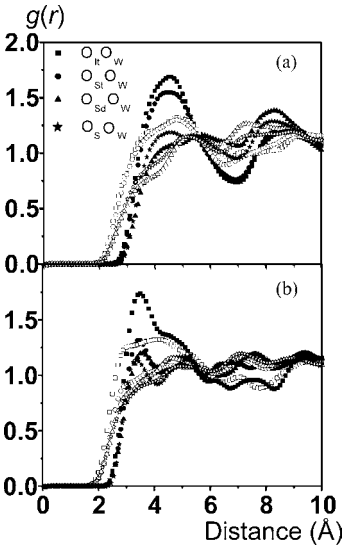

Figure 3. Radial distribution functions, $g(r)$, from the oxygen atoms in the intersection (O_{It}), straight (O_{St}), and sinusoidal (O_{Sd}) channels of silicalite-1 to oxygen (O_W, filled symbols) and hydrogen (H_W, unfilled symbols) atoms of water molecules for the loadings of (a) 1 and (b) 8 water molecules per intersection.

shoulder of the O_S-H_W RDFs while their first peaks appear at the same position.

3.1.1.2. Separated RDF for Each Channel. To understand more details of the water behavior in different channels, the O_S-O_W and O_S-H_W RDFs for each channel have been evaluated. The results are given as examples in Figure 3a and 3b for $n_{ld} = 1$ and 8, respectively. Here, the notation O_s representing oxygen atoms of the silicalite-1 surface is replaced by O_{It}, O_{St}, and O_{Sd} for intersection, straight, and sinusoidal oxygen atoms, respectively. Average O_S-O_W and O_S-H_W RDFs for both loadings are also given for comparison. The following conclusions can be extracted from the plots.

In terms of the peak height, which gives information regarding the probability of finding water molecules present in the investigated channel, the detected order is intersection > straight > sinusoidal. This conclusion is valid for the RDFs from the silicalite-1 surface to both oxygen and hydrogen atoms of water and both $n_{ld} = 1$ and 8. The averaged O_S-O_W and O_S-H_W RDFs cannot be compared with those of the individual channels because the number density, $\rho = n/V$ (where n is the number of water molecules moving in each channel and V denotes the volume of the simulation cube), is not known for each channel. Therefore, the individual RDFs are normalized to the total number of water molecules in the simulation cube, N. In other words, the y-axis for the channel-specific RDFs is in arbitrary units. However, the peak position does not depend on the number density. What we learn from these facts is that the height of the $O_{St}-O_W$ RDFs is similar to those of $O_{It}-O_W$ for $n_{ld} = 1$ (Figure 3a) and of $O_{Sd}-O_W$ for $n_{ld} = 8$ (Figure 3b). At low loadings, the probability of detecting water molecules in the intersection and straight channels is considerably higher than that for the sinusoidal channel, that is, diffusion along the straight channel is superior. The trajectory density plot for $n_{ld} = 1$ shown in Figure 4 confirms this statement. To the contrary, no significant difference has been found for $n_{ld} = 8$ in the diffusion of water molecules along straight and sinusoidal channels.

Considering the RDFs in Figure 3 in terms of the peak positions and their shapes, all plots for the separate RDFs are almost identical to those of the averaged ones (for both concentrations and both types of RDFs). The only different RDF is for $O_{Sd}-O_W$. In addition to the first peak at 4.2 Å of the averaged O_S-O_W RDF, the separate $O_{Sd}-O_W$ RDF shows a second peak at 5.6 Å. The appearance of this peak can be

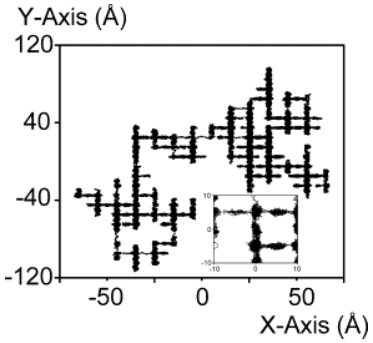

Figure 4. Projection onto the xy plane of the 10-ns trajectory of a water molecule traveling along silicalite-1 channels at $n_{ld} = 1$ and 298 K, where an enlargement is given in the insert.

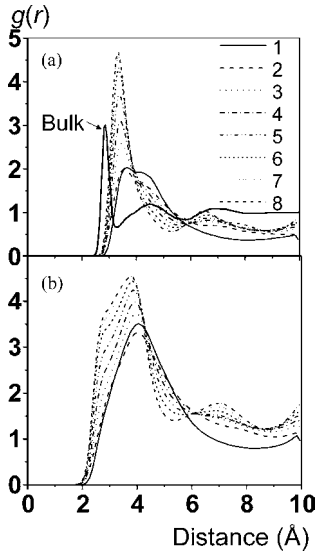

Figure 5. Oxygen−oxygen (a) and oxygen−hydrogen (b) radial distribution functions (RDF) $g(r)$ for water molecules in silicalite-1 at $n_{ld} = 1-8$ (oxygen−oxygen RDF for bulk water taken from ref 29).

TABLE 2: Characteristics of the Radial Distribution Functions for Water Loadings (n_{1d}) of 1−8 Molecules Per Intersection in Silicalite-1[d]

	n_{1d}								
RDF O_WO_W	1	2	3	4	5	6	7	8	bulk[a]
R_{M1}	3.65	3.55	3.45	3.45	3.35	3.35	3.35	3.35	2.80
	4.3[b]	4.3[b]	4.2[b]	4.2[b]					
r_{m1}	8.05	6.45	5.95	5.85	5.65	5.45	5.35	5.25	3.2
n	0.1	0.7	1.2	1.9	2.5	2.9	3.4	3.9	4.5

	n_{1d}								
RDF O_WO_W	1	2	3	4	5	6	7	8	bulk[a]
R_{M1}	4.05	4.05	3.95	3.95	3.85	3.85	3.75	3.75	1.85
r_{m1}	8.45[c]	9.05[c]	8.95[c]	8.75[c]	8.55[c]	5.65	5.45	5.35	2.4
n	1.3	5.7	9.6	11.9	15.8	7.5	8.3	9.2	4.4

[a] Values taken from ref 29. [b] The RDFs show a broad-splitting peak. [c] The RDFs show flat minima. [d] R_{M1} and r_{m1} are the distances in Å for the first maxima and minima of RDFs, respectively, and n is the average coordination number integrated up to r_{m1}.

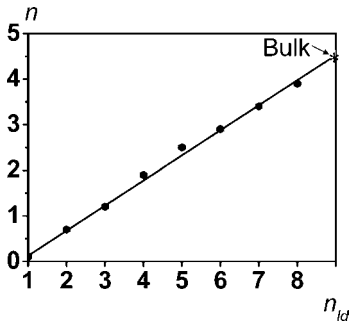

Figure 6. First-shell coordination number, n, as a function of loading, n_{ld} (* stands for that of bulk water taken from ref 29).

attributed to a contribution from the water molecules lying in the other channels. As can be seen from the trajectory density plot (Figure 4), high-density regions in the intersection and sinusoidal channels lie within a spherical shell of radius 5.3 Å with respect to oxygen atoms of the sinusoidal channel. On the other hand, the contributions to the O_{It}–O_W and O_{St}–O_W RDFs are not visible because the water density in the sinusoidal channel is significantly lower than that in the other channels (Figure 3a).

3.1.2. Water−Water Radial Distribution Functions. To gain insight into how water molecules coagulate inside the channels, the RDFs (O_W−O_W) and (O_W–H_W) at a loading of eight water molecules have been calculated (see Figure 5a and 5b, respectively). The O_W–O_W RDF for pure water is also given for comparison. Characteristics for the pronounced peaks of the RDFs are summarized in Table 2.

3.1.2.1. The Oxygen−Oxygen Radial Distribution Function. Comparing the structure of bulk water and of water inside silicalite-1, significant differences in the water structure are seen. The O_W−O_W RDF for pure water shows a typical first peak at 2.80 Å, a second peak at 4.50 Å, and a first shell coordination number (n) of 4.5 water molecules.[29] Inside the cage, the O_W−O_W RDF changes dramatically as a function of loading. With the concentration of eight water molecules per intersection, the plot shows a first sharp peak at 3.35 Å, a minimum at 5.25 Å, and $n = 3.9$ water molecules. The distances to the first maxima (R_{M1}) and the first minima (r_{m1}) increase steadily if the concentration decreases. In addition, peak splitting starts to be detected at $n_{ld} = 4$ and the peaks separate at $n_{ld} = 1$. This indicates the changes of water structure in the cage of silicalite-1. The appearance of the first sharp peak for high loading is assigned to the formation of water clusters in the cage of silicalite-1 (details in the next paragraph) while the split peak for low loading, especially for $n_{ld} = 1$, at 4.5 Å is interpreted as due to water molecules separated into different channels.

In terms of first-shell coordination numbers, a linear relation with the water concentration has been detected and plotted in Figure 6. The coordination number of 3.9 for the loading of eight water molecules per intersection is close to that of 4.5 for pure water.[29]

The O_W−O_W RDFs for pure water and for a high concentration of water in the silicalite-1 cage, especially for $n_{ld} = 8$, have similar shapes and their first-shell coordination numbers are about the same. It is known that bulk water forms a hydrogen bond network with an O−O distance, indicated by the first peak of the O_W−O_W RDF, of 2.80 Å. Therefore, it is evident from the O_W−O_W RDF of water molecules in the cage of silicalite-1, at least for $n_{ld} = 8$, that clusters are formed. Characteristics of the cluster can be figured out from the RDFs and summarized as follows: (i) Water molecules in the cluster in the cage of silicalite-1 do not hydrogen bond with one another because the O−O distance of 3.35 Å (R_{M1} of the O_W−O_W RDF for $n_{ld} = 8$) is about 0.5 Å longer than the typical hydrogen bond distance in bulk water. This does not appear to fit the geometrical and the energetic criteria[30−32] of hydrogen bond formation. (ii) The height of the O_W−O_W RDF indicates that the water clusters in the cage of silicalite-1 are less flexible than those of pure water. This observation can be understood in terms of their interactions with water molecules in the second solvation shell and with the silicalite-1 wall. Because of the limited space in the channel, the second solvation shell of water does not form (the second peak at about 6.5 Å of the O_W−O_W RDF shown in Figure 5a for other loadings is due to the water molecules lying in different channels). This leads to a destruction of the hydrogen-bonding networks and, hence, a lower stability of the water clusters in the cage of silicalite-1 in comparison with those of pure water. Destructive contributions can be compensated by the interaction with the silicalite-1 wall in which the first shell molecules can be weakly held in place by the water/silicalite-1 potential. We conclude that the stability, which leads consequently to the sharp and pronounced O_W−O_W first peak at 3.35 Å, is due to destructive and constructive contributions from the second solvation shell and the silicalite-1 wall, respectively. (iii) On the basis of the detailed description given in (ii), the size of the "low-density water clusters" in terms of the spherical radius, r_{sphere} (equivalent to R_{M1} of the O_W−O_W RDF), is expected to depend strongly on Δr (the difference between the radius of the pure water cluster and of the silicalite-1 channels), that is, r_{sphere} increases as a function of Δr. This should be contrary to what is seen in small channel zeolites where "high-density water clusters" (R_{M1} of the O_W−O_W RDF < 2.80 Å) are seen.

In contrast, the most recent work of Demontis et al.[17] observes the first peak of the O_W−O_W RDF at approximately 2.80 Å (at 300 K and the loading of only two water molecules per silicalite intersection) which is almost the same position as that of bulk water. This indicates that water molecules in the silicalite-1's cage were supposed to spend appreciable time in contact. Some doubts arise when the force-field potential, where the parameters are adjusted to yield the experimental value, such as the diffusion coefficient, was used to represent the interaction between silicalite-1 and water while the ab initio based potentials was employed for the water/water interaction. Therefore, the observation of the O_W−O_W first peak at 2.80 Å would be a contribution to an unbalance of the two interaction potentials, that is, the first pair overestimates the overall interactions. This is in contrast to our simulation in which the ab initio derived potentials for both pairs of interaction have been applied, that is, our models yield practically a one-to-one correspondence between the predicted (by the potential function) and the observed (by the ab initio calculation) interaction energies.

3.1.2.2. Oxygen−Hydrogen Radial Distribution Function. Additional characteristics of the low-density cluster of water molecules in the silicalite-1 cage can be extracted from the O_W−H_W RDFs, shown in Figure 5b. In good agreement with those of O_W−O_W RDFs, the plots for high loadings show a pronounced shoulder centered at about 2.8 Å. This shoulder is less pronounced when the concentration decreases and disappears for $n_{ld} = 1$. The appearance of the first pronounced O_W−H_W shoulder at a shorter distance than that of the first main O_W−O_W peak implies that H_2O....H−OH is superior. This hydrogen bondlike configuration confirms the formation of low-density clusters of water. As already mentioned, the distances to the shoulder of about 2.8 Å and to the first main peak of the O_W−H_W RDFs ranging from 3.75 Å to 4.05 Å for $n_{ld} = 1$−8, are

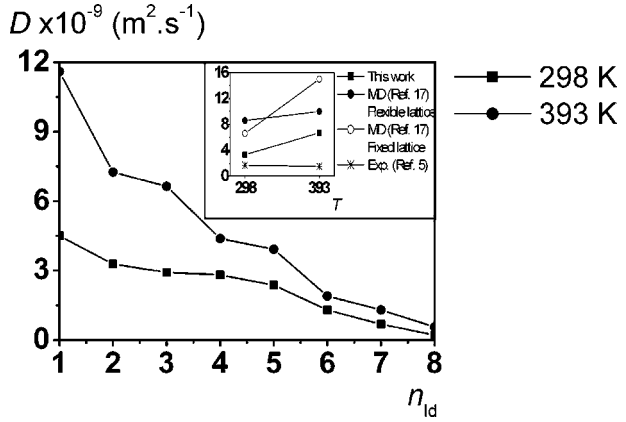

Figure 7. Self-diffusion coefficients (D) as a function of loading (n_{ld}) at 298 and 393 K where experimental values by PFG NMR[5] and the most recent simulation[17] at $n_{ld} = 2$ are given in an insert.

much bigger than what one would expect for a hydgrogen-bonding system.

3.2. Dynamical Properties. 3.2.1. Self-Diffusion Coefficients. The process of self-diffusion can be described by the propagator $P(\mathbf{r},\mathbf{r}_0,t)$ which represents the probability density to find a particle at position $\mathbf{r}$ at time t if it was at $\mathbf{r}_0$ at time $t = 0$.[33] The self-diffusion coefficients are calculated from the moments of this propagator,[34] where the nth moment is defined by the relation[34]

$$\langle|\mathbf{r} - \mathbf{r}_0|^n\rangle = \int|\mathbf{r} - \mathbf{r}_0|^n P(\mathbf{r},\mathbf{r}_0,t)\,\mathrm{d}\mathbf{r} \qquad (2)$$

$P(\mathbf{r},\mathbf{r}_0,t)$ is the solution of the diffusion equation for the initial concentration $C(\mathbf{r},t = 0) = \delta(\mathbf{r} - \mathbf{r}_0)$. The elements of the diffusion tensor, corresponding to the x-, y-, and z-axes, are calculated separately. The overall diffusivity D is one-third of the trace of the diffusion tensor.

The self-diffusion coefficients of the water molecules as a function of the loading, varying from one to eight water molecules per intersection and at 298 and 393 K, are shown in Figure 7. Experimental values by PFG-NMR measurements[5] and the most recent simulations[17] at the loading of two water molecules per intersection are also given in an inset of this figure for comparison. The HF/6-31G* interaction energy at the most stable configuration of -4.5 kcal·mol^{-1} overestimates the MP2/6-31G* of -3.8 kcal·mol^{-1},[16] which can lead to slightly underestimating the simulated diffusion coefficient. However, our values overestimate the experimentally observed self-diffusivities of water by PFG-NMR by approximately a factor of 2 at 298 K and of 4 at 393 K but the discrepancies are less than those taken from ref 17 for both rigid and flexible lattices. An unexpected decrease of experimental values when the temperature increases was already explained in ref 5 in terms of the contributions of extra- and intracrystalline water to the signals measured by PFG-NMR. However, this character has recently been observed for the diffusion of ethane in cation-free zeolite type A at a high temperature and expected for the diffusion of spherical molecules, that is, argon, in cation-free zeolite type A and Y.[35]

Changes of the water self-diffusion coefficients as a function of the loading can be seen from Figure 7. Similar to other small guest molecules such as CH_4, CF_4, He, Ne, Ar, Xe, and SF_6 in silicalite-1,[36] the diffusion of water decreases if the concentration increases. As expected, the diffusivities for all concentrations at 393 K are higher than those at 298 K. The temperature dependence is stronger at low concentrations, that is, the difference of the diffusion coefficients obtained from the two temperatures has almost disappeared at the loading of eight water molecules per interaction.

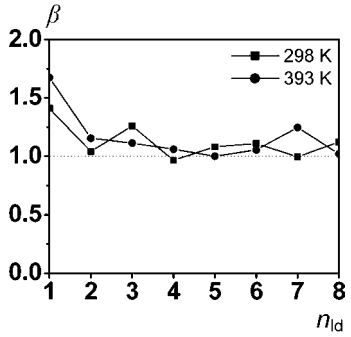

Figure 8. Changes of β (detailed in eq 4) as a function of loading (n_{ld}) at 298 and 393 K.

3.2.2. Anisotropic Diffusion. It has been observed both experimentally and theoretically that the diffusion of alkanes and light gases in silicalite-1 is anisotropic.[37] To visualize this effect, a formula for the relation between the components of the diffusivity tensor (D) proposed by Kärger[38] has been applied:

$$\frac{c^2}{D_z} = \frac{a^2}{D_x} + \frac{b^2}{D_y} \qquad (3)$$

where a, b, and c are the unit cell lengths. The deviation from eq 3 can be accounted for by introducing a parameter,

$$\beta = \frac{c^2/D_z}{(a^2/D_x + b^2/D_y)} \qquad (4)$$

where $\beta = 1$ denotes random processing, for example, a water molecule passing an intersection continues the diffusion path independent of how it gets to the intersection. A sign that a preferentially continuative diffusion path mechanism is active, along in the same channel type, is $\beta > 1$. Vice versa, higher diffusivity in the z-direction ($\beta < 1$) is only possible by changes between straight and sinusoidal channels. The interchange between the two channel types is more probable in this case.

Figure 8 shows the computed β as a function of loading at the two temperatures. As expected, the βs for almost all concentrations and temperatures are higher than 1, indicating the preferential continuation diffusivity of the water molecule in the same silicalite-1 channels. This is in good agreement with studies for xenon and alkane molecules in silicalite-1 in which $\beta = 1.2$ and 1.3 have been inferred.[37] However, as the changes of the β values as a function of loading and temperature derived in the present paper are within the level of fluctuations, relations between these variables cannot be concluded.

The fact that continuation diffusivity is stronger among nonpolar molecules in comparison with polar molecules in silicalite-1 could be due to the reason that the diffusion of a polar molecule is more strongly influenced by its interaction with the silicalite-1 inner surface. Polar molecules are expected to approach closer to the channel wall than nonpolar ones. Therefore, when a polar molecule enters an intersection from a channel of type A, it might be more likely to enter the closest pore, which belongs to the channel of type B (pores to the same type of channel are almost on opposite sides of the intersection) for less continuation diffusivity. This leads directly to a decreased probability of polar molecules taking the same channel type, that is, β for polar molecules is lower than that of nonpolar molecules.

4. Conclusions

We have reported results from a series of MD simulations using ab initio fitted models for water in silicalite-1 at various concentrations at 298 and 393 K. As expected, the observed self-diffusion coefficient increases as a function of temperature and decreases as a function of loading. The change of the water structure is indicated by the O_S-O_W RDFs in which the transition takes place between the loadings of 6 and 7 water molecules per intersection. At high loadings ($n_{ld} = 8$), the interior water molecules configure into unique clusters in the constrained silicalite-1 cage, hence, the destruction and reformation of hydrogen-bonding networks among water molecules and interior silicalite-1. Such "low-density water cluster" shows evidence of a typical behavior of water in silicalite-1 confinements. The difference of the diffusion coefficients obtained from the two temperatures has almost disappeared at the loading of eight water molecules per intersection.

Acknowledgment. The authors thank Prof. Dr. Giuseppe B. Suffritti for the stimulating discussions and Dr. David Ruffolo for proofreading the manuscript. Computing facilities provided by the Austrian−Thai Center for Chemical Education and Research at Chulalongkorn University, Thailand, and the Computing Center at Leipzig University, Germany, are gratefully acknowledged. This work was financially supported by the Royal Golden Jubilee Scholarship of the Thailand Research Fund, Grant No. PHD/0090/2541, and the Deutsche Forschungsgemeinschaft Grant No. FR 1486/1.

Note Added after ASAP Posting. This article was released ASAP on 10/11/2003. Due to a production error, an incorrect version of Figure 5 was published. The correct version was posted on 10/20/2003.

References and Notes

(1) Viswanadham, N.; Shido, T.; Sasaki, T.; Iwasawa, Y. *J. Phys. Chem. B* **2002**, *106*, 10955.
(2) Perez-Ramirez, J.; Mul, G.; Kapteijn, F.; Moulijn, J. A.; Overweg, A. R.; Domenech, A.; Ribera, A.; Arends, I. W. C. E. *J. Catal*. **2002**, *207*, 113.
(3) Ferrari, A. M.; Neyman, K. M.; Mayer, M.; Staufer M.; Gates, B. C.; Rösch, N. *J. Phys. Chem. B* **1999**, *103*, 5311.
(4) Turov, V. V.; Brei, V. V.; Khomenko, K. N.; Leboda, R. *Microporous Mesoporous Mater*. **1998**, *23*, 189.
(5) Bussai, C.; Vasenkov, S.; Liu, H.; Böhlmann, W.; Fritzsche, S.; Hannongbua, S.; Haberlandt, R.; Kärger, J. *Appl. Catal., A* **2002**, *232*, 59.
(6) Demontis, P.; Suffritti, G. B.; Quartieri, S.; Fois, E. S.; Gamba. A.; Morosi, G. *Mater. Chem. Phys.* **1991**, *29*, 357.
(7) Demontis, P.; Suffritti, G. B.; Quartieri, S.; Fois, E. S.; Gamba, A. *Zeolites* **1987**, *7*, 522.
(8) Leherte, L.; André, J. M.; Derouane, E. G.; Vercauteren, D. P. *Comput. Chem.* **1991**, *15*, 273.
(9) Leherte, L.; Lie, G. C.; Swamy, K. N.; Clementi, E.; Derouane, E. G.; André, J. M. *Chem. Phys. Lett.* **1988**, *145*, 237.
(10) Faux, D. A. *J. Phys. Chem. B* **1999**, *103*, 7803.
(11) Cicu, P.; Demontis, P.; Spanu, S.; Suffritti, G. B.; Tilocca, A. *J. Chem. Phys.* **2000**, *112*, 8267.
(12) Termath, V.; Haase, F.; Sauer, J.; Hutter, J.; Parrinello, M. *J. Am. Chem. Soc.* **1998**, *120*, 8512.
(13) Vigné-maeder, F.; Auroux, A. *J. Phys. Chem.* **1990**, *94*, 316.
(14) Turov, V. V.; Brei, V. V.; Khomenko, K. N.; Leboda, R. *Microporous Mesoporous Mater*. **1998**, *23*, 189.
(15) Bopp, P.; Jancso, G.; Heinzinger, K. *Chem. Phys. Lett.* **1983**, *98*, 129.
(16) Bussai, C.; Hannongbua, S.; Haberlandt, R. *J. Phys. Chem. B* **2001**, *105*, 3409.
(17) Demontis, P.; Stara, G.; Suffritti, G. S. *J. Phys. Chem. B* **2003**, *107*, 4426.
(18) Bussai, C.; Fritzsche, S.; Hannongbua, S.; Haberlandt, R. *Chem. Phys. Lett.* **2002**, *354*, 310.
(19) Olson, D. H.; Kokotailo, G. T.; Lawton, S. L.; Meier, W. M. *J. Phys. Chem.* **1981**, *85*, 2238.
(20) Lemberg, H. L.; Stillinger, F. H. *J. Chem. Phys.* **1975**, *62*, 1677.
(21) Stillinger, F. H.; Rahman, K. *J. Chem. Phys.* **1978**, *68*, 666.
(22) Odutola, J. A.; Dyke, T. R. *J. Chem. Phys.* **1980**, *72*, 5062.
(23) Mulliken, R. S. *J. Phys. Chem.* **1962**, *36*, 3428.
(24) Swope, W. C.; Anderson, H. C.; Berens, P. H.; Wilson, K. R. *J. Chem. Phys* **1982**, *76*, 637.
(25) Demontis, P.; Suffritti, G. B. *Chem. Rev.* **1997**, *97*, 2845.
(26) Wolf, D.; Keblinski, P.; Phillpot, S. R.; Eggebrecht, J. *J. Chem. Phys.* **1999**, *110*, 8254.
(27) Dufner, H.; Kast, S. M.; Brickmann, J.; Schlenkrich, M. *J. Comput. Chem.* **1997**, *18*, 660.
(28) Hensen, F.; Cheethan, A. K.; Stockenhuber, M.; Lercher, J. A. *J. Chem. Soc., Faraday Trans*. **1998**, *94*, 3759.
(29) Rahman, A.; Stillinger, F. H.; Lemberg, H. L. *J. Chem. Phys.* **1975**, *63*, 5223.
(30) Marti, J. *J. Chem. Phys*. **1999**, *110*, 6876.
(31) Yoshii, N.; Yoshie, S.; Mira, S.; Okazaki, S. *J. Chem. Phys*. **1998**, *109*, 4873.
(32) Kalinichev, A. G.; Bass, J. D. *J. Phys. Chem.* **1997**, *101*, 9720.
(33) Kärger, J.; Pfeifer, H.; Heink, W. In *Principles and Applications of Self-diffusion Measurements by Nuclear Magnetic Resonance*; Advances in Magnetic Resonance, Vol. 12; Academic Press: New York, 1988.
(34) Fritzsche, S.; Haberlandt, R.; Kärger, J.; Pfeifer, H.; Heinzinger, K. *Chem. Phys. Lett.* **1992**, *198*, 283.
(35) Schüring, A.; Auerbach, S. M.; Fritzsche, S.; Haberlandt, R. *J. Chem. Phys.* **2002**, *116*, 10890.
(36) Skoulidas, A. I.; Sholl, D. S. *J. Phys. Chem. B* **2002**, *106*, 5058.
(37) Maginn, E. J.; Bell, A. T.; Theodorou, D. *J. Phys. Chem.* **1996**, *100*, 7155.
(38) Kärger, J. *J. Phys. Chem.* **1991**, *98*, 5558.